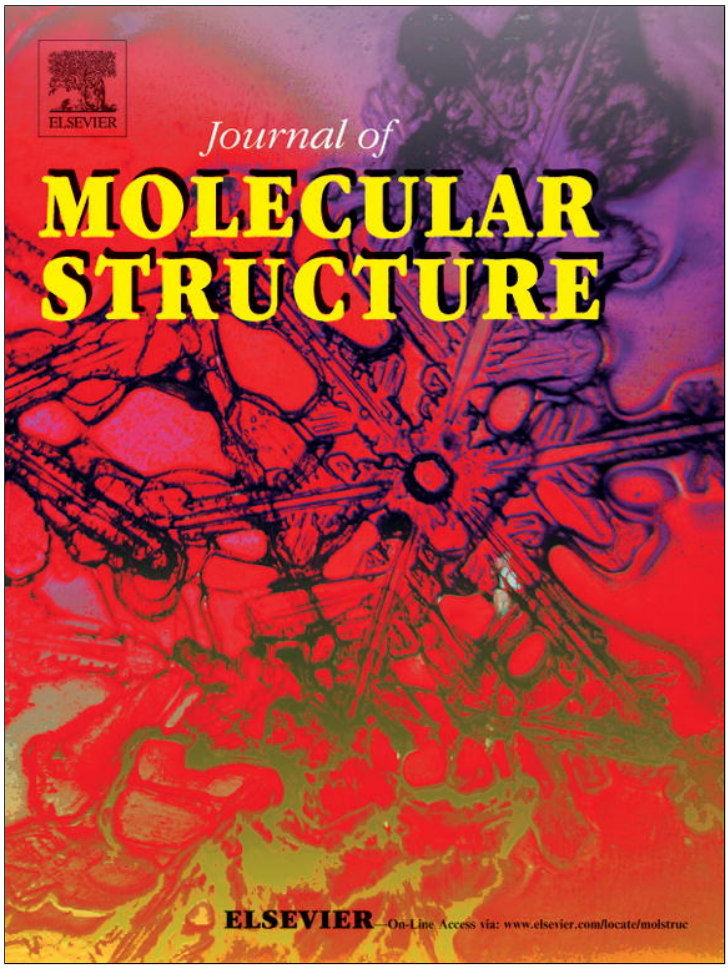

Journal of Molecular Structure 1040 (2013) 83–89

Contents lists available at SciVerse ScienceDirect

Journal of Molecular Structure

journal homepage: www.elsevier.com/locate/molstruc

Solid state modifications of drospirenone

Marián Parisi [a], Eleonora Freire [a,b,*,1], Marcia Rusjan [c], Juan Marcelo Moreno [c], Hernán Bonadeo [a], Daniel Vega [a,b]

[a] Gerencia de Investigación y Aplicaciones, Centro Atómico Constituyentes, Comisión Nacional de Energía Atómica, Av. Gral Paz 1499, 1650 San Martín, Buenos Aires, Argentina
[b] Escuela de Ciencia y Tecnología, Universidad Nacional General San Martín, Martín de Irigoyen 3100, 1650 San Martín, Buenos Aires, Argentina
[c] Laboratorios Raffo-Monte Verde S.A., Agustín Álvarez 4145, B1603APO, Villa Martelli, Buenos Aires, Argentina

HIGHLIGHTS

- The solid state modifications of Drospirenone (DP) are discussed.
- The structure analysis of the crystalline phase of DP is presented.
- The thermal behaviour of DP (crystalline and amorphous) was studied.
- IR and Raman spectra were recorded and the vibrational properties were calculated.

GRAPHICAL ABSTRACT

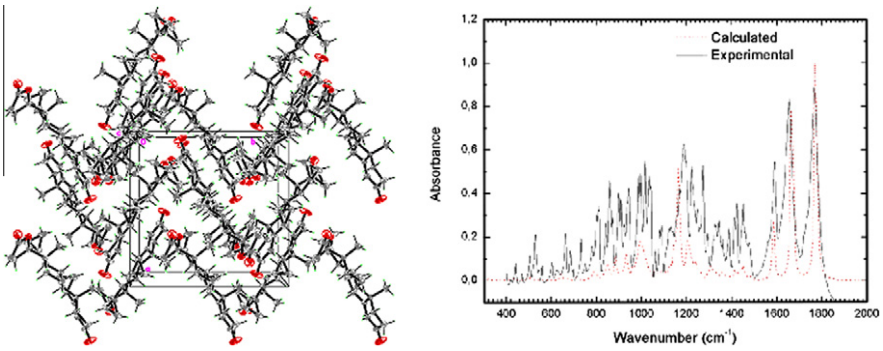

ARTICLE INFO

Article history:
Received 12 October 2012
Received in revised form 18 January 2013
Accepted 18 January 2013
Available online 19 February 2013

Keywords:
Drospirenone
Progestogen
Crystal structure
Amorphous

ABSTRACT

This manuscript presents a structural, thermal and spectroscopic characterization of two different solid state forms of drospirenone (C24 H30 O3), a crystalline phase and an amorphous one. The molecule contains three fused six-membered rings and two five-membered rings; none of them is planar in character.

An intra-molecular hydrogen bond was observed in the crystalline phase. Although the melting point is 202(1) °C, only very weak interactions could be considered responsible for the packing in the crystal.

The amorphous phase was obtained from molten material and was found five times more soluble than the crystalline one.

Infrared and Raman spectra for both phases were recorded and the vibrational properties were calculated using the GAUSSIAN 03 software package; overall agreement between calculations and experiment was obtained.

1. Introduction

Organic compounds can crystallize in more than one crystal form [1], ability known as polymorphism. In some cases, the substance can also be obtained in amorphous phase as a different solid state modification. If this happens in pharmaceuticals, their physical properties such as density, melting point, solubility and then stability, bioavailability and processability will be different. The importance of knowing the different solid state modifications for pharmaceutical industry lies on having reliable and robust processes [2,3].

Drospirenone ((6*R*,7*R*,8*R*,9*S*,10*R*,13*S*,14*S*,15*S*,16*S*,17*S*)-1,3′,4′,6,6a,7,8,9,10,11,12,13,14,15,15a,16-hexadecahydro-10,13-dimethyl-spiro-[17*H*-dicyclopropa-6,7:15,16]cyclopenta[a]phenanthrene-17,2′(5*H*)-furan]-3,5′(2*H*)-dione, see Scheme 1 and from now on DP) is an analogue of the aldosterone antagonist, spironolactone, and is a unique progestogen [4].

* Corresponding author. Address: Departamento Física de la Materia Condensada, GIyA, GAIyANN, Centro Atómico Constituyentes, Comisión Nacional de Energía Atómica, Av. Gral Paz 1499, 1650 San Martín, Buenos Aires, Argentina. Tel.: +54 11 6772 7097; fax: +54 11 5772 7121.
E-mail address: freire@tandar.cnea.gov.ar (E. Freire).
[1] Member of Consejo Nacional de Investigaciones Científicas y Técnicas, Conicet.

0022-2860/$ - see front matter © 2013 Elsevier B.V. All rights reserved.
http://dx.doi.org/10.1016/j.molstruc.2013.01.040

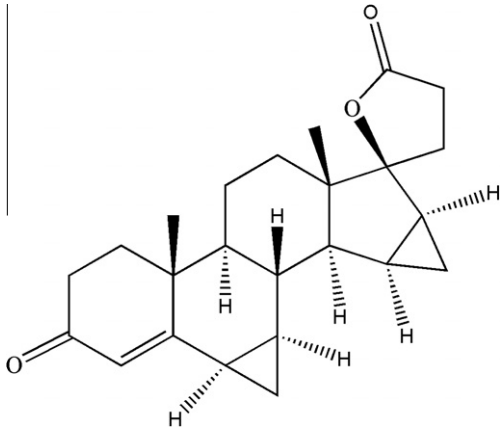

Scheme 1.

The pharmacologic profile of DP is more closely related to that of progesterone, especially with regard to antimineralocorticoid and antiandrogenic activities, than that of any other synthetic progestogen [5–8]. This suggests that adverse effects commonly observed with combination oral contraceptives may be decreased with oral contraceptives containing DP. In fact, the contraceptive efficacy and adverse effects of DP/ethinyl estradiol combination treatment were evaluated with favourable results [9,10]. Additionally, it relieves menstrually related symptoms (e.g., negative affect and water retention) which are commonly observed with other combination oral contraceptives [11].

DP is practically insoluble in water (less than 3 mg/l) and so belongs to class II of the Biopharmaceutics Classification Systems (BCSs). Consequently, studies on the different solid state modifications are essential in this compound due to the possible effects on the bioavailability, as any change in the solid state will have a direct impact on the solubility.

In the present work we have focused our interest on the study of different solid state modifications (amorphous and crystalline) of DP by fully characterization through differential scanning calorimetry, X-ray powder diffraction, single crystal X-ray diffraction and Infrared and Raman spectroscopy.

2. Experimental section

2.1. Materials and methods

DP starting material was provided by Laboratorios Raffo-Monte Verde S.A. Crystalline DP was obtained by crystallization from ethanol at room temperature (25(2) °C). Amorphous material was produced in two different ways: by cooling down to room temperature molten material of crystalline phase and by pouring DP/acetone solution into boiling water.

X-ray powder diffraction (XRPD) patterns were recorded on a X'Pert Philips PW3020 diffractometer over the 2θ range of 5–40°, using graphite monochromatized Cu Kα radiation (1.54184 Å), in aluminium sample holders, at room temperature (1°. divergence slit; 1°. detector slit and 0.1 mm receiving slit, scanning step 0.02°., counting time 2 s). Suitable samples for XRPD measurement were obtained by grinding crystalline or amorphous material in an agate mortar, achieving particle size around 5 μm.

Differential scanning calorimetry (DSC) was carried out with a Shimadzu DSC-60 instrument. Samples weighting 3–5 mg were heated in opened aluminium pans at a rate of 10 K/min under nitrogen gas flow of 35 mL/min.

Table 1
Crystal and experimental data of drospirenone.

Formula	$C_{24}H_{30}O_3$
Formula weight	366.48
Crystal size (mm)	0.50 × 0.33 × 0.25
Crystal system	Orthorhombic
Space group, Z	$P2_12_12_1$, 4
a (Å)	12.236(2)
b (Å)	12.592(2)
c (Å)	12.879(2)
Volume (Å^3)	1984.2(5)
Absorption coef (mm^{-1})	0.079
Density (calc., gr/cm^3)	1.227
Melting point (°C)	202(2)
No. of reflections	
measured/unique	8188/4164
with $I > 2\sigma(I)$	2975
R_{int}	0.04
Parameters/restraints	244/0
Measurement	Gemini A, Eos CCD detector
θ_{max} (°)	28.9
$R[F^2 > 2\sigma(F^2)]$	0.0561
$wR(F^2)$	0.136
GOF on F^2	1.054
$\Delta\rho_{max}/\Delta\rho_{min}$ (eÅ^{-3})	0.21/−0.24
Flack parameter	1(2) Absolute structure determined by synthesis

Polarized thermomicroscopy was performed using an Instec HCS302 hot stage in a Zeiss Axioskip 40 microscope and an on-purpose adapted Nikon Digital Sight DS-U1 camera.

2.2. X-ray crystallography

Single-crystal X-ray diffraction: X-ray Data was collected using a Gemini Oxford diffractometer with an EOS CCD area detector and CrystAlisPro software [12], with graphite-monochromated Mo Kα (λ = 0.71073 Å) at 293(2) K. The structures were solved by direct methods using SHELXS-97 [13] and all of the non-hydrogen atoms were refined anisotropically by full-matrix least-squares on F^2 using SHELXL-97 [13]. Those H atoms attached to C were placed at calculated positions (C—H: 0.98 Å, C—H_2: 0.97 Å and C—H_3: 0.96 Å) and allowed to ride. Displacement factors were taken as $U(H)_{isot}$ = 1.2/1.2/1.5 U_{host}.

Absolute structure could not be determined from diffraction data, but it is known from synthesis. All calculations were performed using WinGX [14] and Ortep-3 for windows [15]. Crystal and experimental data are listed in Table 1 and the corresponding structures are shown in Figs. 1–3.

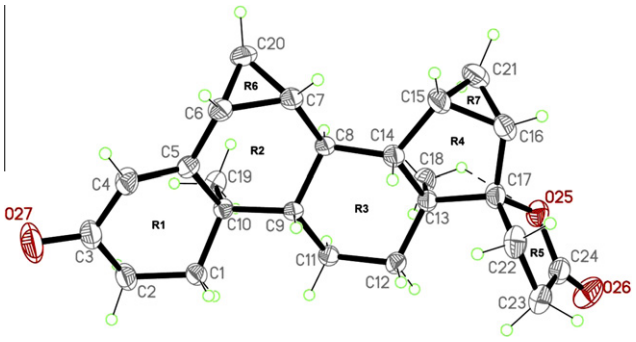

Fig. 1. The molecular structure of DP showing the atom-numbering scheme. Displacement ellipsoids are drawn at the 50% probability level and H atoms are shown as small spheres of arbitrary radii. The intra H-bond C18—H18A...O25 is shown as dashed line.

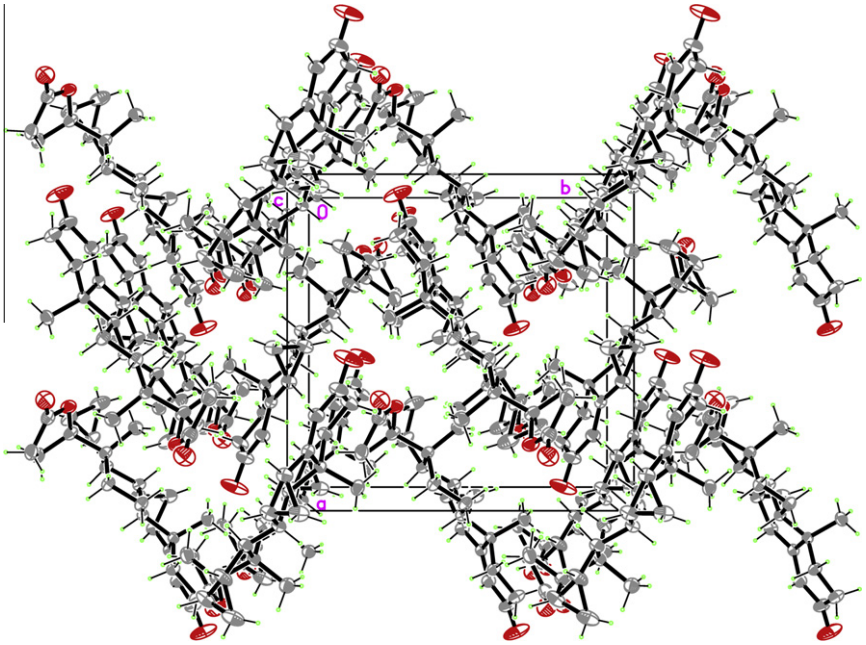

Fig. 2. The packing diagram of DP showing a zigzag arrangement of molecules.

2.3. Spectroscpic methods

The *vibrational spectra* of DP in the internal band region, for both the amorphous and the crystalline forms, were measured using a NICOLET 8700 Fourier Transform infrared spectrometer. The powder samples were dispersed in KBr pellets and the IR spectra were recorded in the 400–4000 cm^{-1} wavenumber region; the resolution was 4 cm^{-1}.

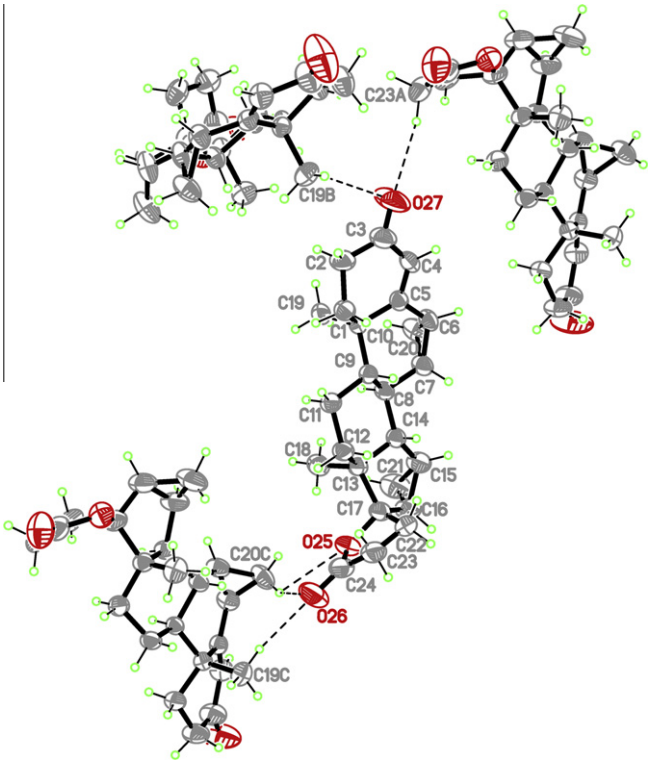

Fig. 3. Very weak hydrogen bonding interactions showing electronegative O atoms into electropositive environment from neighbors.

The *Raman spectra* of crystalline and amorphous DP from 100 to 3600 cm^{-1} were recorded with a LabRAM HR (Horiba Jobin Yvon) Raman instrument with a 632.82 nm laser as the exciting line.

UV–Visible spectra were measured using a Perkin Elmer Lambda 25 UV/Vis spectrometer in the 200–500 nm range with a quartz recipient having a 1 cm optical pathway.

Saturated water solutions: saturated solutions of crystalline and amorphous materials were generated by placing an excess amount of sample (52 mg) in 500 ml of water. These suspensions were stirred for 2 h at room temperature (25(2) °C) and the final suspensions were filtered using 0.45 μm Millipore filter. No extra dilution was necessary.

2.4. Vibrational calculations

Ab initio density-functional theory (DFT) calculations [16,17] on the single molecule have been carried out using the B3LYP functional, which makes use of Becke′s 3-parameter exchange functional [18] and the Lee–Yang–Parr correlation functional [19]. It has been shown that among the available functionals the B3LYP one yields a good description of harmonic vibrational frequencies of organic molecules. We chose the widely used 6-31G++G(d,p) basis set [20], which contains *d* polarization functions on heavy atoms and *p* polarization on hydrogen atoms.

The molecular structure obtained from single crystal X Ray Diffraction was used as starting model for computational calculations, an energy optimization was performed.

Harmonic vibrational wavenumbers were calculated analytically, and IR intensities were obtained within the double harmonic approximation [21], ignoring cubic and higher force constants as well as omitting second and higher dipole moment derivatives. Raman scattering cross sections for each normal mode are calculated from polarizability derivatives. These are Gaussian broadened and the intensity spectrum thus obtained is normalized to the strongest observed peak for comparison. The homogeneous scale factor for calculated vibrational wavenumbers was set to 0.9619 [22] throughout. The spectral curves of the IR absorbance are the sum of Gaussian shaped bands obtained from calculated IR Absorption intensities. All ab initio calculations have been carried out using the GAUSSIAN 03 program package [23].

3. Results and discussion

3.1. Structure analysis

Crystalline DP has one molecule of drospirerone in the asymmetric unit. The molecule (Fig. 1) contains three fused six-membered rings (R1, R2 and R3). Moreover, two five-membered rings (R4 and R5) are also present in the molecule, one of them (R4) fused to ring R3. None of them is planar in character. Besides, two three-membered rings, R6 and R7, are fused to rings R2 and R4 respectively.

Searching in the CSD [24] for crystal structures with similar rings (from R1 to R4), a great number of hits were found; two of them were observed as the most similar to DP (refcodes GENTAV [25] and QORBIJ [26]). However, ring R6 is not present in GENTAV and ring R5 is absent in QORBIJ. The most evident difference between these structures and that of DP is observed in the relative position of the ring R1, probably due to different configurations. While QORBIJ and GENTAV show sp3 character on C4, DP exhibits an sp^2 one. Bond distances and angles on C4 are listed in Table 2, while C5—C4, C4—C3 and C5—C4—C3 are 1.505 Å, 1.486 Å and 112.63° for GENTAV and 1.533 Å, 1.523 Å and 115.3° for QORBIJ respectively. Due to this difference, R1 is puckered as an envelope on C1 in DP (Q = 0.444(4) Å, θ= 58.1(5)°, Φ = 354.8(7)°) [27] while it is puckered as a chair in QORBIJ and GENTAV. Moreover, C5 shows sp3 character in QORBIJ (C5—C4 1.533 Å, C5—C6 1.517 Å, C5—C10 1.568 Å) but sp^2 character in DP (see Table 2). This is the reason why R1 protrudes from the R2, R3 and R4 mean plane in QORBIJ and the molecule is folded.

The other two six-membered rings, R2 and R3, can be described as a half-chair and a chair respectively (Q = 0.484(4) and 0.608(4) Å, θ = 50.3(5) and 4.1(4)°, Φ = 249.0(6) and 272.7(5)° for R2 and R3 respectively) [27]. Besides, the two five-membered rings, R4 and R5, are puckered as an envelope on C13 and a twisted conformation on C17—C22 respectively (Q = 0.399(5) and 0.286(6) Å, Φ = 179.8(6) and 242.6(5)° for R4 and R5 respectively).

The general packing (Fig. 2) can be described as a zigzag of molecules. An intra-molecular hydrogen bond was observed (C18—H18A···O25, see Table 3 and Fig. 1). No other relevant hydrogen bonds could be found. However, as it will be mentioned later on, the compound melts above 200 °C, a relatively high melting point for an organic compound where only Van der Waals interactions are present. Inspecting the packing, it is possible to observe electropositive zones of the DP molecule approaching electronegative ones of neighbouring molecules (see Fig. 3). In fact, O25 and O26 are surrounded by hydrogen atoms from C20 and C18, and O27 by hydrogen atoms from C19 and C23. Although these interactions are very weak, they have sometimes been considered in the packing description [28], and they are also considered here as weak hydrogen bonds responsible for packing interactions in this crystal structure (see Table 3).

Table 2
Selected geometric parameters (Å, °) of drospirenone.

C2—C3	1.488(4)
C3—O27	1.224(4)
C3—C4	1.443(4)
C4—C5	1.346(4)
C5—C6	1.470(4)
C5—C10	1.523(3)
O27—C3—C4	122.2(3)
O27—C3—C2	120.6(3)
C4—C3—C2	117.2(3)
C5—C4—C3	124.7(3)
C4—C5—C6	118.8(2)
C4—C5—C10	121.2(2)
C6—C5—C10	119.9(2)
C3—C4—C5—C10	−3.3(4)

Table 3
Hydrogen-bond parameters (Å, °) of drospirenone.

D—H···*A*	*D*—H	H···*A* *A*	*D*···*A*	*D*—H···*A*
C18—H18A···O25	0.96	2.32	2.782(4)	109.0
C20—H20A···O25^{i}	0.97	2.87	3.404(4)	115.9
C19—H19B···O26^{i}	0.96	2.67	3.574(4)	157.7
C20—H20A···O26^{i}	0.97	2.66	3.513(4)	146.9
C23—H23B···O27^{ii}	0.97	2.46	3.422(4)	169.2
C19—H19A···O27^{iii}	0.96	2.78	3.722(4)	167.9

Symmetry codes: $^{i}-x-1/2, -y-1, z-1/2$; $^{ii}-x-3/2, -y-1, z+1/2$, $^{iii}x+1/2, -y-3/2, -z$.

The obtained structural model was used to calculate the X-ray powder diagram (Fig. 4, pattern d), which reproduces the experimental diagrams for commercial bulk material or for our sample obtained by recrystallization from acetone solution by slow evaporation (Fig. 4, patterns c and b respectively).

3.2. Thermal analysis

Thermal behaviour of DP (recrystallized material) was studied by DSC analysis and the results are introduced in Fig. 5 (trace b).

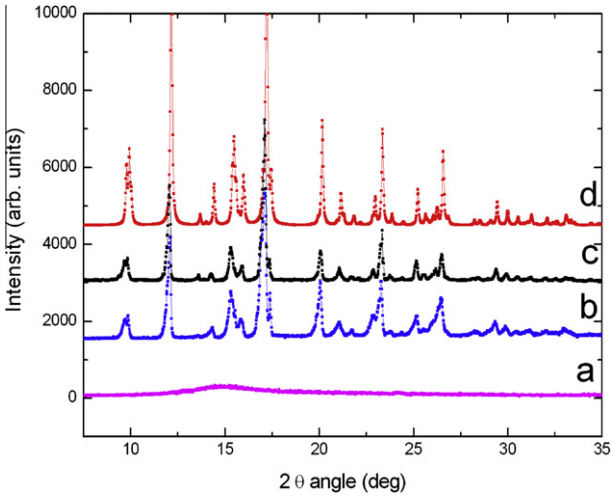

Fig. 4. X-ray powder patterns: (a) amorphous phase, (b) sample obtained from acetone, (c) commercial bulk material and (d) calculated pattern.

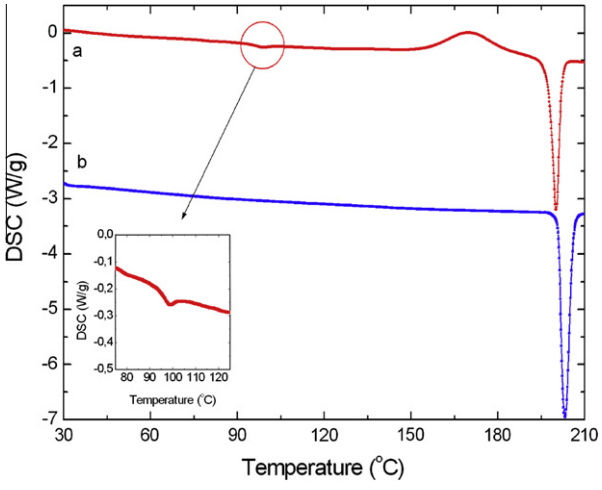

Fig. 5. DSC analysis of DP. Trace (a): amorphous phase showing glass transition (see insert), exothermic recrystallization and melting. Trace (b): crystalline phase showing melting temperature at 202(1) °C.

The melting temperature was determined at 202(1) °C and the phase transition involves an enthalpy change of 72(4) J/g with no decomposition. The molten material was supercooled to study any possible recrystallization event, but an amorphous phase was obtained. The amorphous character was determined both by optical microscopy, where it was possible to confirm the absence of birefringence, and by X-ray diffraction (Fig. 4, pattern a), where no peaks were observed in the pattern.

The thermal behaviour of the DP amorphous phase was also studied by DSC analysis (see Fig. 5, trace a) where three different thermal events were observed. At 95(3) °C a change in the base line is observed (see insert in Fig. 5, trace a) corresponding to a glass transition. After that, above 155 °C, an exothermic event is detected, where the amorphous material suffers a recrystallization process. Finally, at 199(2) °C an endothermic event is observed, with an enthalpy change of 63(5) J/g. This last event was linked to the melting point of the obtained crystal phase when the thermal behaviour was followed by thermal microscopy.

The previously described thermal events were also followed by XRPD. The main results are described in Fig. 6, where a crystal phase (Fig. 6, pattern c) was used as starting material. The sample was melted and then quenched, showing the typical amorphous pattern (Fig. 6, pattern a). This amorphous material was heated to 180 °C and then quenched. The sample obtained in such a way is crystalline in character and the XRPD pattern is presented in Fig. 6, pattern b, showing that this final material is similar to the starting one, and thus confirming that the amorphous phase crystallizes into the same initial crystal phase after the exothermic event. The melting temperature of this last material seems to be slightly smaller than the starting one.

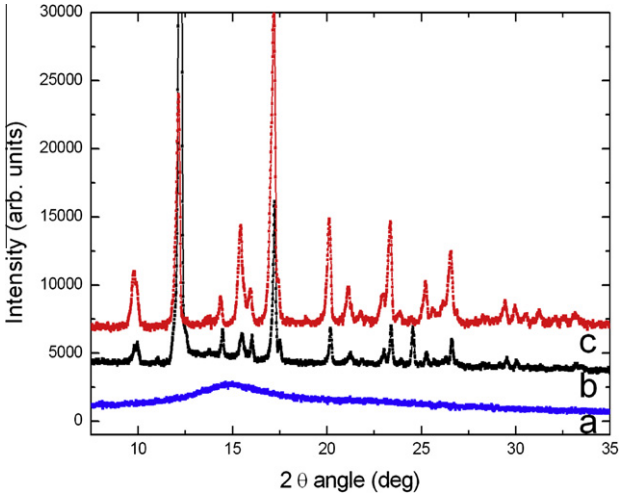

Fig. 6. XRPD studies for samples quenched at different temperatures. Pattern (a) quenched after melting, amorphous phase; pattern (b) quenched at 180 °C, recrystallized from the amorphous phase; pattern (c): starting material.

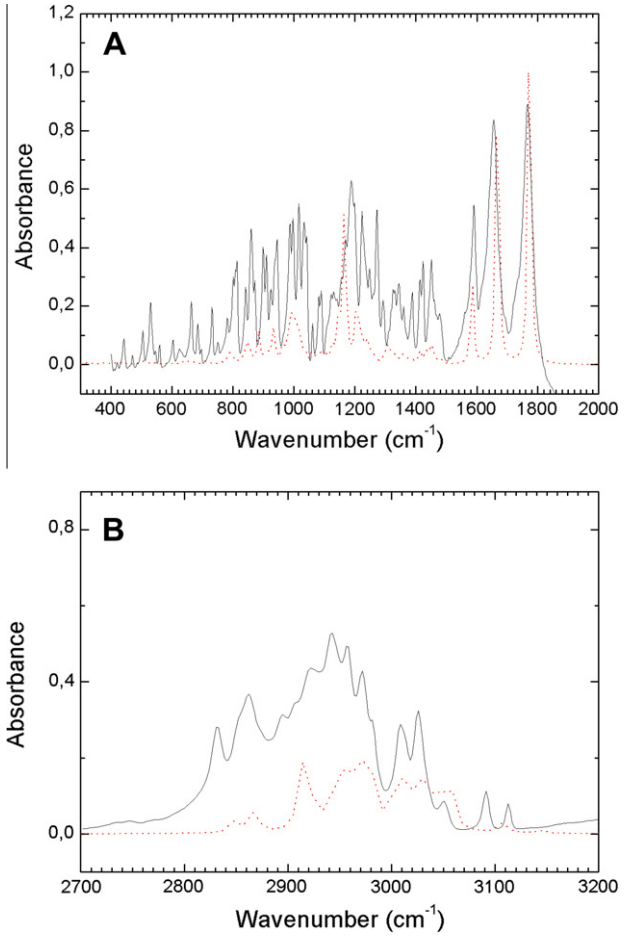

Fig. 7. (A) IR spectra of DP from experiments (full line) and calculations (dashed line) in the region of 400–2000 cm^{-1}. (B) IR spectra of DP from experiments (full line) and calculations (dashed line) in the region of 2700–3200 cm^{-1}.

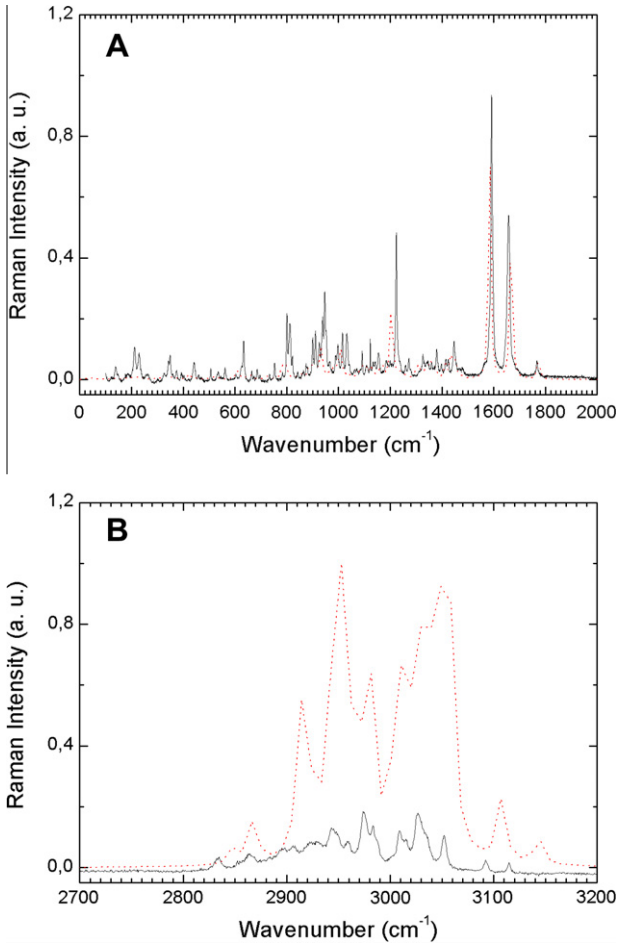

Fig. 8. (A) Raman spectra of DP from experiments (full line) and calculations (dashed line) in the region of 100–2000 cm^{-1}. (B) Raman spectra of DP from experiments (full line) and calculations (dashed line) in the region of 2700–3200 cm^{-1}.

3.3. Vibrational analysis

The DP molecule has no symmetry, and its 165 normal modes are IR and Raman active; the same occurs in the amorphous state. The factor group of the crystal is D_2, and it has 4 molecules in the unit cell; the modes are split into four factor group components: three are IR active and all four Raman active.

Although is rather unusual, IR and Raman spectra of both crystalline and amorphous phases are very similar. The intermolecular interaction, which could cause band broadening for the amorphous state, and factor splitting in the crystal, are small. This is the reason why calculations based on a single molecule, rather than much more complicated crystal calculations have been performed in this work. Similarly, only spectra of the crystalline phase are presented. Fig. 7a and b shows the IR spectrum and Fig. 8a and b the Raman spectrum of the crystal.

In general, the frequencies of the experimental Raman and Infrared bands are very close, as predicted. Starting from high wavenumbers, we observe the complex pattern of the CH stretching vibrations from 3200 to 2800 cm^{-1}. Proceeding to lower energies, the region between 1900 and 1500 cm^{-1} is dominated by normal modes associated with double bonds, two C=O stretching and a C=C stretching. In both cases experimental and calculated spectra cluster around the same frequencies range and seem to be consistent. In particular three strong bands at 1766, 1655 and 1591 cm^{-1} are observed in the infrared spectrum, but only two of this group are strong in the Raman spectrum; the 1766 cm^{-1} band being very weak. The bands at 1766 and 1655 cm^{-1} are raised from C24O26 and C3O27 carbonyl stretching modes respectively. The 1591 cm^{-1} band is due to C4C2 double bond stretching vibration. Fig. 9 shows the excellent agreement between calculations and experiment for both Raman and Infrared spectra. Continuing to lower energies, we reach the *fingerprint region*, where detailed assignment of vibrational modes to observed peaks is difficult. The range between 1550 and 1000 cm^{-1} corresponds to C—H bending modes; at lower frequencies these mix with ring motions; below 800 cm^{-1} the bands correspond to C—C stretchings from the rings.

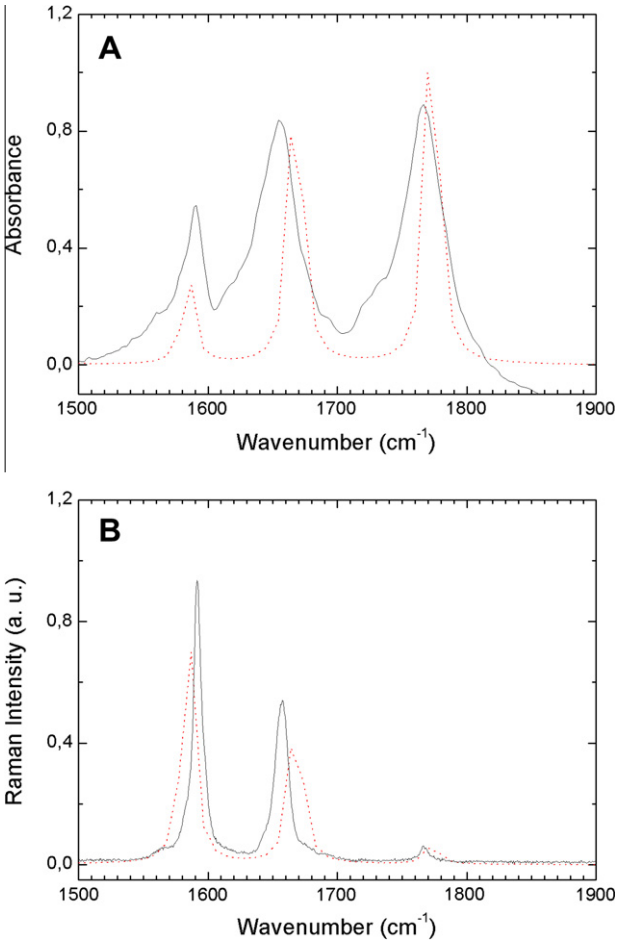

Fig. 9. Detail of (A) IR and (B) Raman spectra from experiments (full line) and calculation (dashed line) of DP in the double bond region.

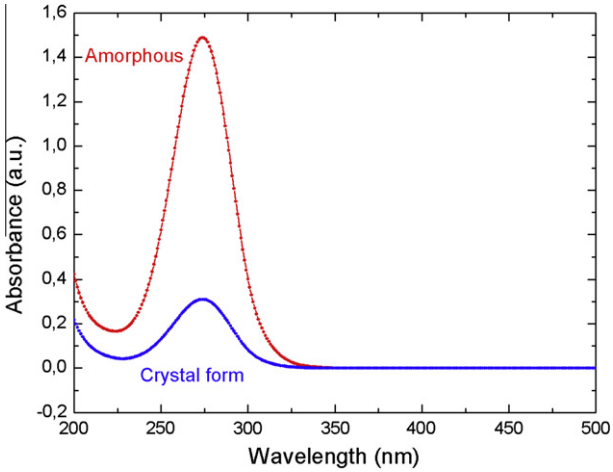

Fig. 10. Relative solubility study. UV–visible determinations from saturated water solutions of amorphous phase and crystal form.

Comparing the experimental spectra with the calculated ones, a reasonable correlation is observed taking into account the complexity of the molecule.

3.4. Solubility

It could be useful to point out here that amorphous phases are very difficult to detect. Moreover, they belong to high energetic materials so the impact on the solubility will always be important. In this context, we determined the relative solubility of amorphous and crystalline phases by UV–visible measurements of saturated water solutions. Fig. 10 shows that the amorphous phase is around five times more soluble than the crystalline one.

4. Conclusions

Summarizing, this manuscript presents a structural, thermal and spectroscopic characterization of two different solid states of DP, a crystalline phase and an amorphous one. The amorphous phase is a high energetic material so is expected to be less stable than the crystalline one. Although no systematic study on stability was performed, the amorphous character was confirmed before every test. The amorphous phase proved to be stable at room temperature for the time the different experiments lasted (typically 2 or 3 days) and also when it was ground in a mortar to generate powder. Although the amorphous phase can also be obtained by pouring a DP/acetone solution into boiling water or by dropping the solution onto a hot plate, in general a mixture of amorphous and crystalline phases was obtained following these procedures.

Acknowledgements

We thank the financial support of CONICET (PIP N° 00889), ANPCyT (Project No. PME 2006-01113) for the purchase of the Oxford

Gemini CCD diffractometer and the Spanish Research Council (CSIC) for provision of a free-of-charge licence to the Cambridge Structural Database. We acknowledge B. Halac's help with the Raman measurements and also thank J. Rodríguez and R. Weht for their helpful assistance with vibrational calculations.

Appendix A. Supplementary material

CCDC 903900 contains the supplementary crystallographic data for DP. These data can be obtained free of charge from The Cambridge Crystallographic Data Centre via www.ccdc.cam.ac.uk/data_request/cif. Supplementary data associated with this article can be found, in the online version, at http://dx.doi.org/10.1016/j.molstruc.2013.01.040.

References

[1] S.R. Byrn, in: Solid State Chemistry of Drugs, Academic Press, New York, 1982.
[2] J. Haleblian, W. McCrone, J. Pharm. Sci. 58 (1969) 911.
[3] M.R. Caira, Top Curr. Chem. 198 (1998) 163.
[4] U. Fuhrmann, R. Krattenmacher, E.P. Slater, K.H. Fritzemeier, Contraception 54 (1996) 243.
[5] P. Muhn, R. Krattenmacher, S. Beier, W. Elger, E. Schillinger, Contraception 51 (1995) 99.
[6] W. Oelkers, V. Berger, A. Bolik, et al., J. Clin. Endocrinol. Metab. 73 (1991) 837.
[7] W. Losert, J. Casals-Stenzel, M. Buse, Arzneimittelforschung 35 (1985) 459.
[8] P. Muhn, U. Fuhrmann, K.H. Fritzemeier, R. Krattenmacher, E. Schillinger, Ann. NY. Acad. Sci. 761 (1995) 311.
[9] K.S. Parsey, A. Pong, Contraception 61 (2000) 105.
[10] R. Krattenmacher, Contraception 62 (2000) 29.
[11] L.L. Breech, P.K. Braverman, Int. J. Womens Health 1 (2009) 85.
[12] CrysAlisPro. Oxford Diffraction Ltd. Version 1.171.33.66. April 2010.
[13] G.M. Sheldrick, Acta Cryst. A 64 (2008) 112.
[14] L.J. Farrugia, J. Appl. Cryst. 32 (1999) 837.
[15] L.J. Farrugia, J. Appl. Cryst. 30 (1997) 565.
[16] R.G. Parr, W. Yang, Density-Functional Theory of Atoms and Molecules, Oxford University Press, New York, 1989.
[17] W. Koch, M.C. Holthausen, A Chemist's Guide to Density Functional Theory, second ed., Wiley-VCH, Weinheim, 2001.
[18] A.D. Becke, J. Chem. Phys. 98 (1993) 5648.
[19] C. Lee, W. Yang, R.G. Parr, Phys. Rev. B 37 (1988) 785.
[20] G.A. Petersson, A. Bennett, T.G. Tensfeldt, M.A. Al-Laham, W.A. Shirley, J. Mantzaris, J. Chem. Phys. 89 (1988) 2193.
[21] D.M. Bishop, Rev. Mod. Phys. 62 (1990) 343.
[22] M.P. Andersson, J. Phys. Chem. A 109 (2005) 2937.
[23] M.J. Frisch et al., GAUSSIAN 03, Revision D.02, Gaussian, Inc., Wallingford CT, 2004.
[24] F.H. Allen, Acta Cryst. B 58 (2002) 380.
[25] Wei Zhou, Wei-Xiao Hu, Chun-Nian Xia, Acta Cryst. E 62 (2006) o4132.
[26] M. Bandini, M. Contento, A. Garelli, M. Monari, A. Tolomelli, A. Umani-Ronchi, E. Andriolo, M. Montorsi, Synthesis (2008) 3801.
[27] D. Cremer, J.A. Pople, J. Am. Chem. Soc. 97 (1975) 1354.
[28] G.R. Desiraju, T. Steiner, The Weak Hydrogen Bond in Structural, Chemistry and Biology, Oxford University Press, 1999.